# The Effect of the Shape of Ischaemic Regions in the Heart on the Resulting Extracellular Epicardial Potential Distributions

JP Barnes, PR Johnston

Griffith University, Brisbane, QLD, Australia

## Abstract

*The majority of recent studies on ischaemia during the ST segment assume that ischaemia progresses from the endocardium to the epicardium and the ischaemic region is rectangular in shape. The presence of sharp edges in these models plays a significant role in the determination of ST segment epicardial potential distributions (EPDs), with current loops forming around these edges. This numerical study looks at ischaemic geometries which remove some or all of the sharp edges and how this affects the resulting EPDs. The two key ischaemic region geometries studied are cylindrical and semi-ellipsoidal in shape.*

*Using a simple anisotropic model for the cardiac geometry and realistic conductivity values, this study shows that cylindrical ischaemic regions give similar results to their rectangular counterparts. However ellispoidal geometries differ, especially at medium levels (30%-70%) of ischaemia, where the EPD splits into 2 depressions instead of the 3 found with the other ischaemic geometries.*

## 1. Introduction

Deviation of the ST segment in the electrocardiogram (ECG) is widely accepted as an indicator of ischaemia in the heart. The mechanisms behind this behaviour however, are not yet fully understood [1] and there is no clear consensus on the measured extracellular epicardial potentials. In recent years, the advancement of computing technology has allowed numerical models to quickly and non-invasively examine scenarios which could not be done by their experimental counterparts. A large amount of this research has been dedicated to understanding the effect of ischaemia on the ST segment of the ECG [2–5]. It is well understood from these numerical studies that full thickness ishemia leads to ST segment elevation over the ischaemic region. For the case where the ischaemic region has not extended to the epicardium, the results begin to vary, due to the differing choices in parameters such as conductivity and fibre rotation. The earliest numerical models [6, 7] used isotropic conductivities and ignored cardiac fibre rotation. Work by Johnston *et al.* [2] however, showed that anisotropy must be incorporated in order to achieve realistic results. The more recent experimental [8] and numerical [4,5] studies using anisotropic conductivity values have shown that at low thickness ischaemia, depression is found over the ischaemic region while at higher thicknesses, elevation occus over the ischaemic region and depression over the ischaemic lateral borders. The different choices of vital parameters between models however resulted in noticable differences for medium levels of ischaemia (30%-70%). One consistent result noticed in these studies was the formation of 'current loops' around the ischaemic region, which arise due to injury currents between tissues of differing transmembrane potential. As these studies all represent the ischaemic region in a 'rectangular' fashion, the sharp corners allow for these loops to form.

The motivation for this study is to see whether these current loops are still apparent in ischaemic geometries which do not possess as many sharp corners and also how this affects the EPDs. For this study three different ischaemic geometries were used: rectangular, cylindrical and semi-elipsoidal. The rectangular ischaemic geometry was used to validate the model against the analyical results by Johnston *et al.* [2] while the other geometries represented decreasing presence of the sharp edges.

## 2. Methods

As this study focusses on the ST segment of the ECG, (the isoelectric phase), the steady state bidomain equation can be employed to find the resulting epicardial potential distributions. It has the following form;

$$\nabla \cdot (M_i + M_e)\nabla\phi_e = -\nabla \cdot M_i \nabla\phi_m \qquad (1)$$

where $M_i$ and $M_i$ are the intracellular and extracellular conductivities and $\phi_e$ and $\phi_m$ are the extracellular and transmembrane potentials, respectively. A simple slab model introduced by Johnston *et al.* [2] was used to represent a ventricle wall. This model considered a 1cm thick insulated slab of ventricular tissue with infinite length and width. The epicardium was situated at $z = 0$ and the endocardium at $z = 1$. A volume of blood of infinite thickness

then sat on top of the tissue. The potential in the blood was governed by the equation

$$\nabla^2 \phi_b = 0 \tag{2}$$

The advantage of using such a model was that for a well chosen size and shape of ischaemic tissue, the model could be solved analytically with the help of fourier transforms. However, as the inversion was done numerically, the dimensions of the slab in the $x$ and $y$ directions needed to be finite. It was found by Johnston *et al.* that a slab 16cm $\times$ 16cm was large enough in order for the potentials to tend to zero at the boundaries. For a more complete description on the slab model including descriptions of the boundary conditions, refer to [2].

The conductivity values used in this study were the same as [2] and were based on the values given by Clerc *et al.* [9]: $\sigma_e^l = 0.625$ S/m, $\sigma_e^t = 0.236$ S/m, $\sigma_i^l = 0.174$ S/m, $\sigma_i^t = 0.0193$ S/m. Also, linear fibre rotation was included with a total rotation from the endocardium to epicardium of 120°. These values were used so that the numerical methods used in this study could be validated against the previously found analytical solutions.

## 2.1. Rectangular ischaemic geometry

For the ischaemic region, the original slab model used a rectangular geometry with a width of 4cm in the $x$ and $y$ directions with the bottom in contact with the endocardium. The ischaemic tissue was defined as having a transmembrane potential 30mV lower than that of normal tissue and a smooth transition from ischaemic to healthy tissue was employed. This was acheived by varying the transmembrane potential from 0mV to -30mV across the border zone according to the equation

$$\phi_m(x, y, z) = -30\Psi(x)\Psi(y)\Psi(1 - z) \tag{3}$$

In each spacial direction, the function $\Psi(p)$ is defined as

$$\Psi(p) = \begin{cases} \dfrac{1 - e^{\frac{-a_p}{\lambda_p}} \cosh \frac{p}{\lambda_p}}{1 - e^{\frac{-a_p}{\lambda_p}}} & |p| \leq a_p \\ \dfrac{e^{\frac{-|p|}{\lambda_p}} \sinh \frac{a_p}{\lambda_p}}{1 - e^{\frac{-a_p}{\lambda_p}}} & |p| > a_p \end{cases} \tag{4}$$

where $a_p$ is the half width of the ischaemic region in the respective spatial direction, measured from the centre of the border zone, and $\lambda_p$ is a parameter to adjust the sharpness of the transition. For this study, similar to previous work, a value of 0.01 was chosen for $\lambda_p$ in all directions.

## 2.2. Cylindrical ischaemic geometry

The cylindrical ischaemic region was constructed to have similar size and border zone properties as the rectangular geometry. The cylinder was constructed with a radius of 2 and the equation for the transmembrane potential was given by

$$\phi_m(r, z) = -30\Psi(r)\Psi(1 - z) \tag{5}$$

where $r$ is in the radial direction and $\Psi$ is defined as in equation (4). All other parameters were kept the same as with the rectangular model to eliminate interference with the results.

## 2.3. Semi-ellipsoidal ischaemic geometry

Like the cylindrical ischaemic zone, the ellipsoidal zone was constructed to have a similar size as the rectangular zone. It was constructed by taking the top hemisphere from an oblate spheroid described by the equation

$$\frac{x^2}{a_r^2} + \frac{y^2}{a_r^2} + \frac{(z-1)^2}{a_z^2} = 1 \tag{6}$$

where $a_r$ is the radius at $z = 1$ and $a_z$ is the vertical, conjugate radius. A value of 2 was chosen for $a_r$ to be consistent with the previous ischaemic geometries. The transmembrane potential was governed by the equation

$$\phi_m(d) = \begin{cases} -15e^{-\frac{d}{\lambda}} & \text{outside ischaemic region} \\ 15e^{-\frac{d}{\lambda}} - 30 & \text{inside ischaemic region} \end{cases} \tag{7}$$

where $d$ is the perpendicular distance to the centre of the border zone and $\lambda$ is again a parameter which controls the sharpness of the transition.

## 3. Results and discussion

For the model using a rectangular ischaemic geometry, the results show that at relatively low thicknesses of ischaemia ($a_z < 30\%$), the epicardial potential distribution has a single depression located directly over the ischaemic region. As the ischaemic thickness is increased, this single depression begins to seperate into three depressions, one remaining above the ischaemic region and two over opposing lateral borders. By the time the thickness reaches $50\%$, the three depressions become quite distinct, as can be seen in figure 1. When the ischaemic thickness is increased above $70\%$, elevation started to occur in the areas between depressions. These areas of elevation quickly consume the region above the ischaemia and once the ischaemic thickness reach $85\%$, the central depression is almost completely replaced with elevation. For a better understanding of this process, it is benificial to look at the the current paths inside the slab model. Figure 2 shows the general behaviour of these current paths for medium ischaemic thicknesses by taking a cross section at $x = 0$.

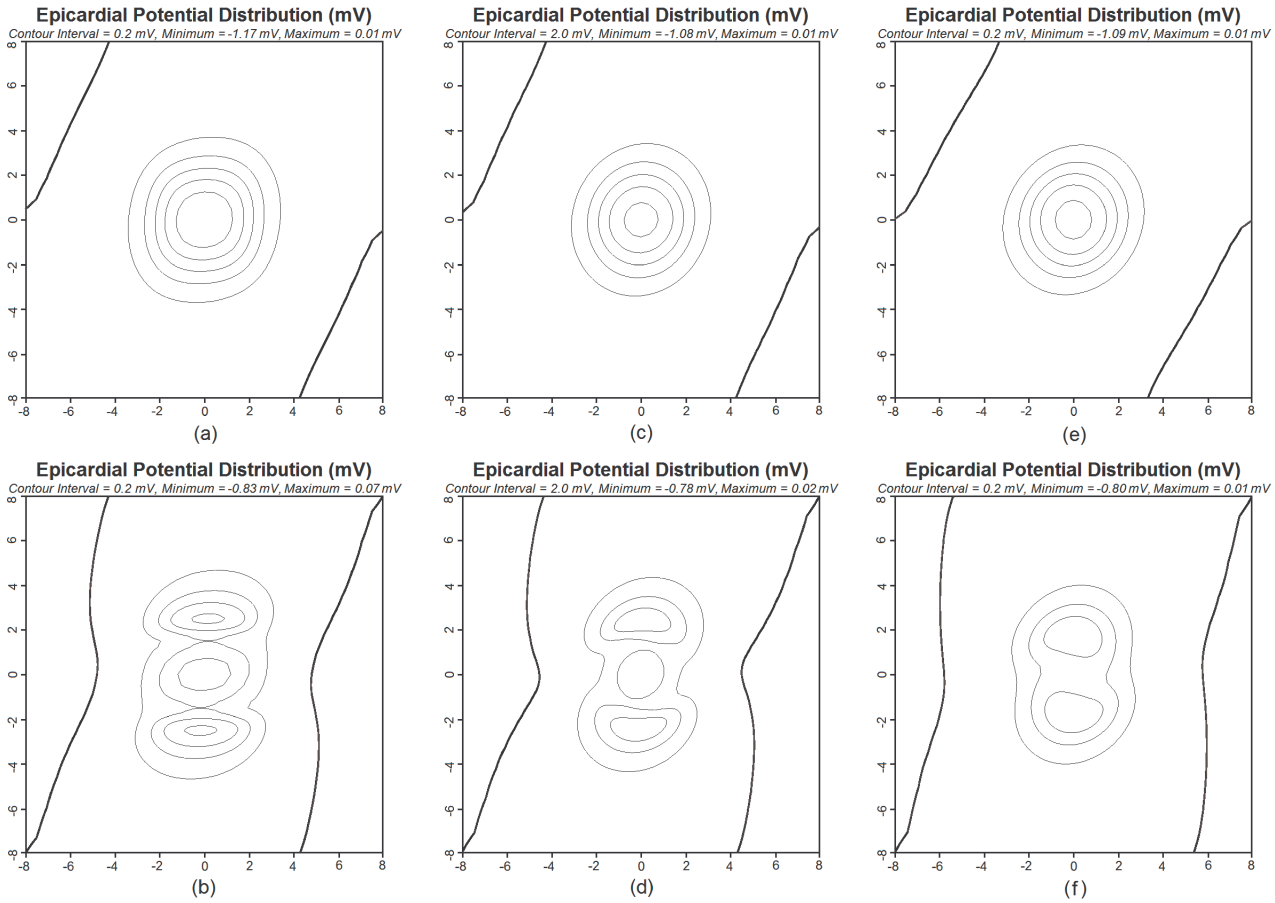


Figure 1. Epicardial potential distriburion for the 3 different ischaemic geometries. The top row has an ischaemic thickness of 10% and the bottom row 50%. The columns from left are the rectangular, cylindrical and ellipsoidal geometries. In each plot, the thick line represents the zero potential (relative to the top right corner) and the thin lines represent negative potentials.

What can be seen from this figure is that at low levels of ischaemia, current loops are formed around the lateral borders of the ischaemic region which rotate towards the centre. This behaviour leads to a current sink in the cente at the epicardium which gives the single depression found in the results. As the ischaemic thickness is increased, a seperate loop forms around the top edge which rotates in the opposite direction to the more dominant loop around the bottom edge. Once the level of ischaemia reaches $30\%$ the effects of the top loop reach the epicardium and this is when the single depression begins to split up. This behaviour continues until the the effects of the top loop star to overpower the bottom loop and this is when positive potentials at the epicardium occur.

Comparing the epicardial distributions for the rectangular and cylindrical ischaemic models, there is not a significant change in the behaviour. The cylindrical model still forms a single depression which then splits into three distinct depressions at approximately the same level of ischaemia. Once the level of ischaemia reaches $70\%$ elevation in the epicardial potentials again occurs which quickly consumes the area above the ischaemic region. There are slight differences between the two geometries, such as the minimum potential in the cylindrical ischaemic model is slightly higher than that of the rectangular model. Overall however, the change in ischaemic shape has not influenced the epicardial potential distributions significantly.

The current paths of the cylindrical ischaemic model also show very similar behaviour to that of the rectangular ischaemic model, with the formation of current loops around the top and bottom sharp edges of the ischaemic zone. This, along with the previous results suggests that it is likely to be the top edges which play the most significant role in determining the epicardial potentials for these models. Comparing the epicardial distributions for the ellipsiodal ischaemic model to the previous two, immediately the differences can be seen. At low levels of ischaemia, the behaviour is quite similar to the previous models, with a sin-

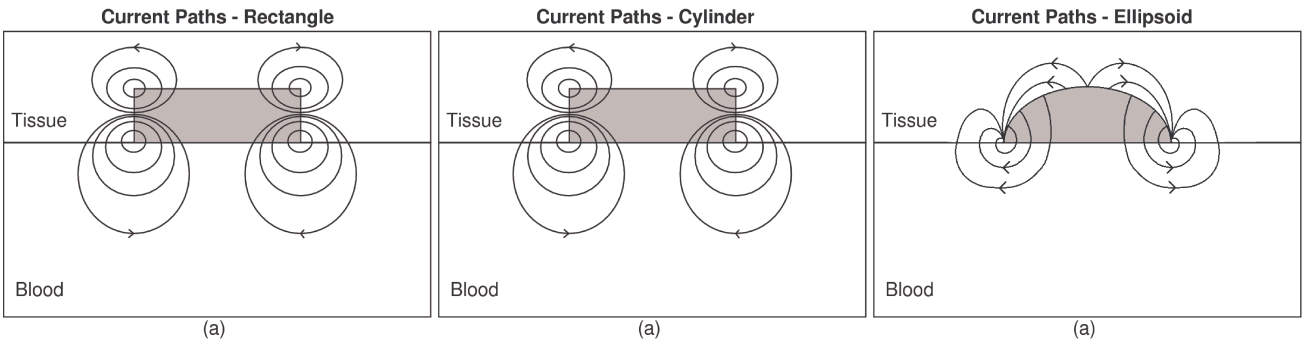


Figure 2. Current paths for the rectangular (a), cylindrical (b) and ellipsiodal (c) geometries at 50% ischaemia. Constructed by taking a cross section at $x = 0$.

gle depression occuring over the ischaemic region. As the ischaemic thickness is increased however, the single depression splits into only two depressions instead of three and again, once the thickness is at $50\%$, the two depressions become quite distinct. At high levels of ischaemia, elevation starts to occur in the area above the ischaemic region which again quickly consumes the entire area. An interesting difference in the ellipsoidal ischaemic model is that that the elevation begins in the centre and moves outward instead of inward as with the previous models. This means that the area of maximum elevation is at the centre of the ischaemic region instead of on the inside of the ischaemic borders.

Looking at the current paths for the ellipsiodal ischaemic model helps to understand the different behaviours noticed. For low levels of ischaemia, the current paths look similar to the previous models, with loops forming around the edges of the ischaemic region. As the ischaemic thickness increases however, the secondary loops found with the previous models no longer form as there are no top edges. The edges of the ischaemic region at the endocardium now act like a current sink, which leads to the two depressions over the edges of the ischaemic region. Once the top of the ischaemic region gets close enough to the epicardium ($70\%$), elevation over the centre occurs due to the current moving outward from the centre.

## 4. Conclusions

The results from this study show that the shape of the ischaemic region has a significant effect on the potential distributions observed at the epicardium. Using three simple geometries for the ischaemic region, it was found that ellipsoidal geometry resulted in significantly different potential distributions on the epicardium for medium thickness ischaemia. This suggests that knowledge of the shape of the ischaemic region is important in understanding the relationship between epicardial potential distributions and ischaemia.

## References

[1] Rodriguez B, Trayanova N, Noble D. Modeling Cardiac Ischemia. Ann NY Acad Sci 2006;1080:395–414.

[2] Johnston PR, Kilpatrick D, Li CY. The Importance of Anisotropy in Modeling ST Segment Shift in Subendocardial Ischaemia. IEEE Trans Biomed Eng 2001;48(12):1366–1376.

[3] Johnston PR, Kilpatrick D. The Effect of Conductivity Values on ST Segment Shift in Subendocardial Ischaemia. IEEE Trans Biomed Eng 2003;50(2):150–158.

[4] MacLeod RS, Shome S, Stinstra J, Punske BB, Hopenfeld B. Mechanisms of Ischemia-Induced ST-Segment Changes. J Electrocardiol 2005;38(4, Suppl. S):8–13.

[5] Potse M, Coronel R, Falcao S, LeBlanc A, Vinet A. The Effect of Lesion Size and Tissue Remodeling on ST Deviation in Partial-Thickness Ischemia. Heart Rhythm 2007; 4(2):200–206.

[6] Holland RP, Brooks H. Spatial and Non-Spatial Influences on TQ-ST Segment Deflection of Ischemia - Theoretical and Experimental Analysis in Pig. J Clin Invest 1977;60(1):197–214.

[7] Smith GT, Geary GG, Blanchard W, Roelofs TH, Ruf W, Mcnamara JJ. An Electrocardiographic Model of Myocardial Ischemic Injury. J Electrocardiol 1983;16(3):223–233.

[8] Li DS, Li CY, Yong AC, Kilpatrick D. Source of Electrocardiographic ST Changes in Subendocardial Ischemia. Circ Res 1998;82(9):957–970.

[9] Clerc L. Directional Differences of Impulse Spread in Trabecular Muscle from Mammalian Heart. Journal of Physiology 1976;255(2):335–346.

Address for correspondence:

Josef Barnes
School of Biomolecular and Physical Sciences, Griffith University, QLD, Australia
josef.barnes@griffithuni.edu.au